International Journal of Pharmacology

Int. J. Pharmacol. **2026**; 22(7): 51059
https://doi.org/10.31083/IJP51059

Review

Advances in Antitumor Drug Development and Mechanistic Studies of the Marine Bisindole Alkaloid Staurosporine

Shangjie Li[1,†], Si Yan[1,2,†], Guangshuai Zhang[1,2], Wenjing He[1], Shuanglin Qin[1,2,*]

[1]National Engineering Research Center of Personalized Diagnostic and Therapeutic Technology, TCM Precision Medicine Research Department, FuRong Laboratory, Hunan University of Chinese Medicine, 410208 Changsha, Hunan, China
[2]Hubei Engineering Research Center of Traditional Chinese Medicine of South Hubei Province, School of Pharmacy, Xianning Medical College, Hubei University of Science and Technology, 437100 Xianning, Hubei, China
*Correspondence: shuanglin@tju.edu.cn (Shuanglin Qin)
[†]These authors contributed equally.
Academic Editor: Mehmet Ozaslan
Submitted: 16 February 2026 Revised: 28 April 2026 Accepted: 20 May 2026 Published: 17 November 2026

Abstract

Staurosporine (STA), originally isolated from *Streptomyces staurosporeus* in 1977, is the earliest known natural indolocarbazole alkaloid. The distinctive structure of STA comprises an indolo[2,3-a]pyrrolo[3,4-c]carbazole core connected via two C-N glycosidic bonds to an aminopyranosyl moiety. As prototypical bisindole alkaloids, STA and its derivatives exhibit significant antitumor activities, with IC_{50} values ranging from nanomolar to micromolar levels against various malignancies, including leukemia, lung carcinoma, breast cancer, and gastrointestinal neoplasms. These compounds exert their anticancer effects through multiple mechanisms, including suppressing tumor cell proliferation via cell cycle arrest, inducing apoptosis through intrinsic and extrinsic pathways, inhibiting tumor cell migration and invasion, and suppressing tumor angiogenesis. Structure-activity relationship (SAR) analyses indicate that modifications at the C-3′ amino position, the C-7 position, the C-3 position, and the glycosidic moiety can significantly improve antitumor efficacy, target specificity, and pharmacokinetic properties. Therefore, STA is considered an exemplary lead compound for rational drug design. This review summarizes the cytotoxicity, mechanisms, SAR, and pharmacological development of STA and its derivatives. Moreover, this review highlights their multimodal and multitarget antitumor characteristics, and aims to provide a theoretical foundation and strategic guidance for clinical translation and the discovery and development of novel drugs based on the indolocarbazole scaffold.

Keywords: staurosporine; antineoplastic agents; drug development; structure-activity relationship

1. Introduction

Cancer remains a major global health issue, characterized by high morbidity, substantial disability, and elevated mortality rates. It currently ranks as the second leading cause of death worldwide, following cardiovascular diseases. According to the World Health Organization, cancer accounts for approximately 10 million deaths annually, representing nearly one-sixth of total global mortality. By 2040, the incidence of cancer globally is projected to rise to approximately 29.9 million cases per year, with corresponding mortality increasing to 15.3 million deaths [1]. Although chemotherapy continues to be the cornerstone of oncological therapy, its clinical application is constrained by several critical limitations. Firstly, many chemotherapeutic agents possess poor aqueous solubility, resulting in low bioavailability and limited drug accumulation at tumor sites, thus restricting their therapeutic index [2]. Secondly, the inherent lack of tumor specificity leads to nonselective toxicity, harming both malignant and normal proliferating cells and causing severe dose-limiting adverse effects [3]. Thirdly, prolonged chemotherapy exposure to chemotherapeutic regimens frequently induces multidrug resistance through various molecular mechanisms, which ultimately leads to treatment failure and disease relapse [4]. Furthermore, elderly oncology patients, who are often characterized by compromised organ function and multiple comorbidities, exhibit reduced tolerance to conventional cytotoxic drugs, thereby significantly increasing the risk of treatment-related toxicities [5]. These limitations substantially reduce the efficacy and safety of current chemotherapy. Therefore, developing novel anticancer agents with improved pharmacological properties remains an urgent priority in contemporary oncology.

The ocean covers approximately 70% of the Earth's surface and supports life across 32 of the 36 recognized animal phyla, establishing itself as a profoundly biodiverse ecosystem often termed the "blue rainforest". Marine organisms biosynthesize structurally and chemically distinct metabolites that are rarely found in terrestrial sources [6]. Marine natural products (MNPs) occupy a broader chemical space than synthetic libraries, thereby providing unique scaffolds to help overcome drug resistance and improve target selectivity. Over the past decade, global pharmaceutical research has increasingly focused on marine bioresources. As of December 2025, 43,856 structurally distinct MNPs have been isolated and characterized. These products encompass seven major chemical classes: terpenoids, alka-

Copyright: © 2026 The Author(s). Published by IMR Press.
This is an open access article under the CC BY 4.0 license.

Publisher's Note: IMR Press stays neutral with regard to jurisdictional claims in published maps and institutional affiliations.

loids, steroids (including steroid saponins), phenolic compounds (including quinones), ethers (including ketones), lactone-containing saponins, and peptides. Pharmacologically, MNPs demonstrate approximately fourfold greater biological activity and lower risk of drug-related liabilities compared to terrestrial counterparts. Currently, at least 34 marine-derived compounds are under clinical evaluation [7]. Among the 20 marine-derived drugs approved by regulatory agencies, 11 are indicated for the treatment of solid tumors or hematological malignancies, reflecting a complete innovation pipeline from marine bioprospecting to bedside clinical application [8].

Marine bisindole alkaloids represent a structurally diverse and pharmacologically important class of MNPs and have emerged as privileged scaffolds in anticancer drug discovery. Distinguished by their structural complexity, broad-spectrum antitumor potency, and unique mechanisms of action, these compounds exhibit substantial potential for clinical translation. Representative chemotypes, including dragmacidins, topsentins, hamacanthins, nortopsentins, fascaplysins, and related bisindole alkaloid families, demonstrate substantially higher clinical translation success rates compared with other natural products [8]. Notably, the newly discovered copper–bisindole alkaloid dimer Chagosendine C illustrates this potential: it induces cuproptosis (copper-dependent cell death) by targeting FDX1. It exhibits nanomolar cytotoxicity against colorectal cancer cells, an *in vivo* tumor growth inhibition rate of 78.2%, and a favorable safety profile [9]. Other marine bisindole alkaloids, including enzastaurin, topsentin derivatives, and dragmacidins, have advanced to clinical or advanced preclinical stages, demonstrating potent efficacy against breast cancer, lung carcinoma, and hematological malignancies. Collectively, these compounds offer distinct advantages in terms of antitumor activity, target selectivity, and multimodal mechanisms. Thus, marine bisindole alkaloids represent important lead structures for overcoming chemoresistance and developing next-generation anticancer therapies.

In recent years, the marine bisindole alkaloid staurosporine (STA) and its synthetic derivatives have become a major focus in medicinal chemistry and pharmacological research. STA was originally isolated from the actinomycete *Streptomyces staurosporeus* by Omura and colleagues in 1977 [10,11]. Its absolute configuration was determined in 1978 by X-ray crystallography, revealing an indolo[2,3-a]pyrrolo[3,4-c]carbazole core linked to an aminopyranose moiety via two C-N glycosidic bonds. The producing strain has undergone taxonomic reclassification twice since its initial discovery: first designated as Saccharothrix aerocolonigenes subsp. AM-2282 in 1995 and later as Lentzea albida in 2002 [12]. STA is among the most potent natural protein kinase inhibitors identified to date, displaying broad-spectrum inhibitory activity against diverse kinases such as protein kinase C (PKC), cyclin-dependent kinases (CDKs), and FMS-like tyrosine kinase 3 (FLT3). However, its nonselective target binding results in dose-limiting toxicities, including cardiotoxicity and myelosuppression, which preclude its direct clinical use [13]. Nevertheless, the exceptional biological potency and favorable structural modifiability of the indolocarbazole scaffold have established STA as a privileged lead structure for rational drug design, with over 55 structurally distinct analogues reported as of 2020 [11]. Strategic modifications at the C-3′ amino position and C-7 hydroxyl group have yielded derivatives with significantly improved kinase selectivity and reduced off-target toxicities [14]. Several STA-derived candidates have progressed to clinical evaluation: lestaurtinib for acute myeloid leukemia (AML); UCN-01, which demonstrates enhanced selectivity for solid tumors, including prostate, breast, and hepatobiliary cancers [15,16]; becatecarin, a rebeccamycin analogue functioning as a dual topoisomerase I/II inhibitor for recurrent small cell lung cancer (SCLC) and metastatic colorectal cancer [17,18]; and edotecarin, a topoisomerase I inhibitor characterized by high stability in the DNA-enzyme cleavable complexes, demonstrating efficacy against gastric cancer, glioblastoma, and colorectal malignancies. These optimized analogues effectively overcome the intrinsic limitations of the parent compound while targeting specific oncogenic kinases (Fig. 1). The FDA approval of midostaurin in 2017 for first-line treatment of FLT3-mutated AML represents a landmark achievement, validating the clinical translational potential of the STA pharmacophore and establishing its role as a cornerstone for next-generation targeted cancer therapeutics [19].

2. Mechanisms of STA-Mediated Antitumor Activity

This study systematically reviews the antitumor mechanisms of STA based on literature published from 1977 to the present (Fig. 2). The review focuses not only on the effects of STA on critical biological processes, including tumor cell proliferation, apoptosis, and metastasis, but also thoroughly explores the associated signaling pathways and molecular mechanisms of STA across diverse cancer types. These findings provide a robust theoretical foundation and practical guidance for future antitumor drug development and clinical applications.

In glioma, STA exerts antiproliferative effects by inducing cell cycle arrest. Studies demonstrated that exposure to 10–50 nM STA for 72 h completely inhibited proliferation of U87MG and U373MG cells, rather than merely delaying it [20]. Different cell lines exhibited distinct cell-cycle responses: U87MG cells were arrested in the S-phase, while U373MG cells accumulated in the G2/M-phase. At the molecular level, STA downregulated CDK2, CDC2, and their cyclin partners (cyclin A and cyclin B1), while concurrently upregulating negative cell-cycle regulators (p21 and p27). However, regulators of the G1 phase (cyclin D1,

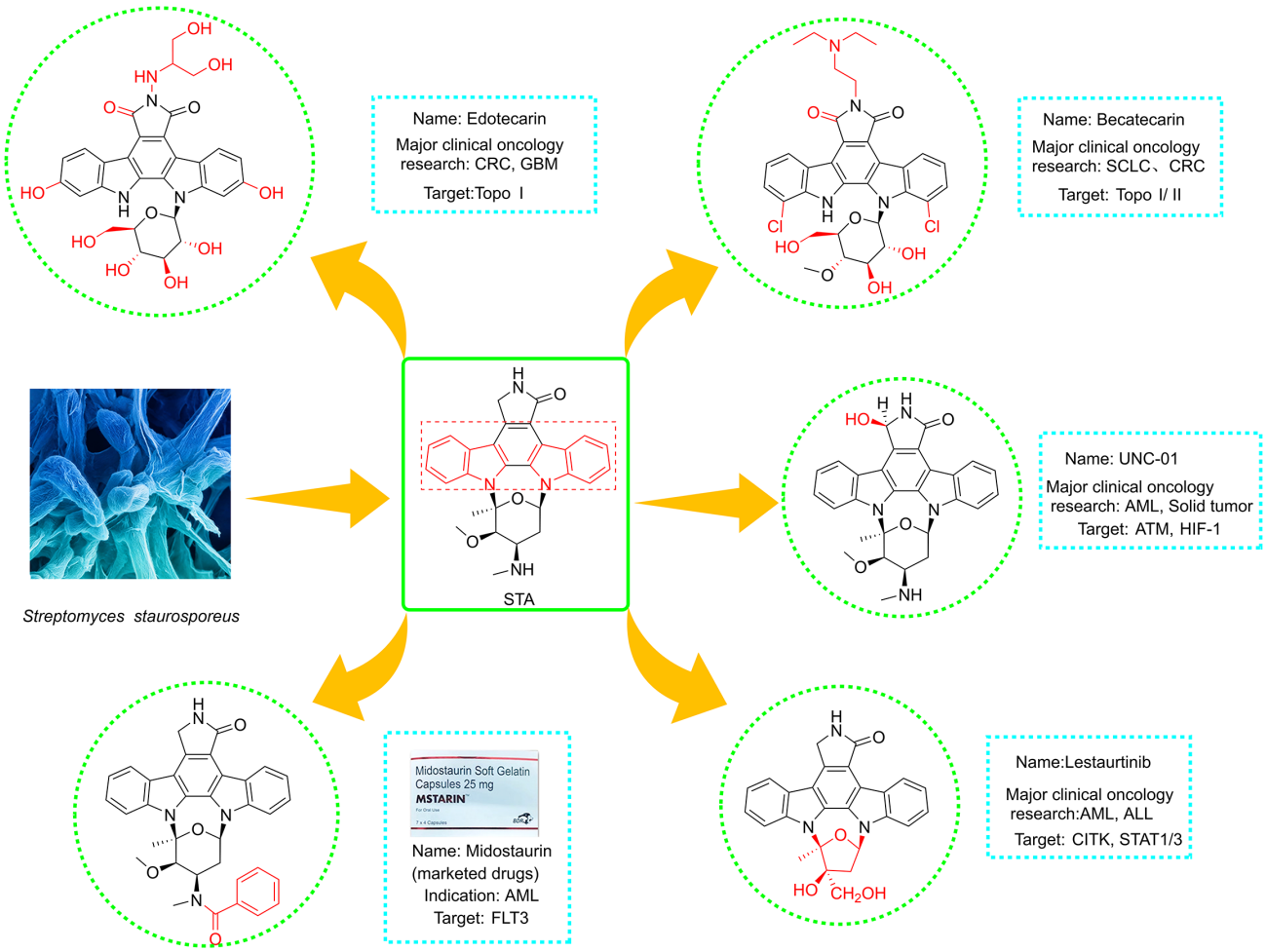

Fig. 1. Chemical structures of staurosporine (STA) and its representative marketed and clinically investigated derivatives.

D3, and CDK4) remained largely unaffected, suggesting that STA primarily disrupts transitions in the S- and G2/M-phases. Research by Baltuch GH et al. [21] demonstrated that glioma cells specifically exhibit elevated PKC activity, which is strongly correlated with proliferation rates ($r = 0.98$). As a potent PKC inhibitor with nanomolar IC_{50} values, STA effectively blocks PKC-mediated proliferative signaling through targeted inhibition [21]. Although PKC inhibition is the classical target of STA, modulation of CDK2 and CDC2 appears more critical. STA not only directly inhibits the catalytic activities of these kinases but also indirectly suppresses them by regulating kinase expression, activation partners, and endogenous inhibitors. This dual mechanism underlies the strong efficacy of STA against glioma.

In melanoma, STA triggers apoptosis via both caspase-dependent and caspase-independent pathways. The early stage involves a classical caspase-dependent cascade: conformational activation and mitochondrial translocation of Bax lead to mitochondrial membrane potential loss, cytochrome c release, and subsequent activation of the caspase-3 and caspase-9, a process partially reversible by pan-caspase inhibitors. Malsy M and colleagues [22] further elucidated the underlying mechanisms using the pancreatic cancer cell lines PaTu8988t and Panc-1. Through STA treatment, they disrupted the pro-apoptotic/anti-apoptotic balance of Bcl-2 family proteins, triggering mitochondrial outer membrane permeabilization (MOMP). Specifically, STA downregulated the anti-apoptotic protein Bcl-2 while promoting the depletion of the BH3-only protein Bad; however, levels of the pro-apoptotic effector Bax remained unchanged. This imbalance resulted in the release of cytochrome c from mitochondria into the cytoplasm, subsequently associating with Apaf-1 to form the apoptosome, which specifically activated caspase-9. Activated caspase-9 then cleaved and activated effector caspase-3, leading to DNA fragmentation, chromatin condensation, and apoptotic body formation, culminating in apoptosis. In later stages, the process transitions to a caspase-independent mode, wherein apoptosis-inducing factor (AIF) translocates directly from mitochondria to the nucleus, ultimately leading to cell shrinkage, chromatin condensation, DNA fragmentation, and apoptotic body formation, thereby completing the programmed cell death process [23]. Overexpression of Bcl-2 delayed early apoptotic events but minimally affected late-

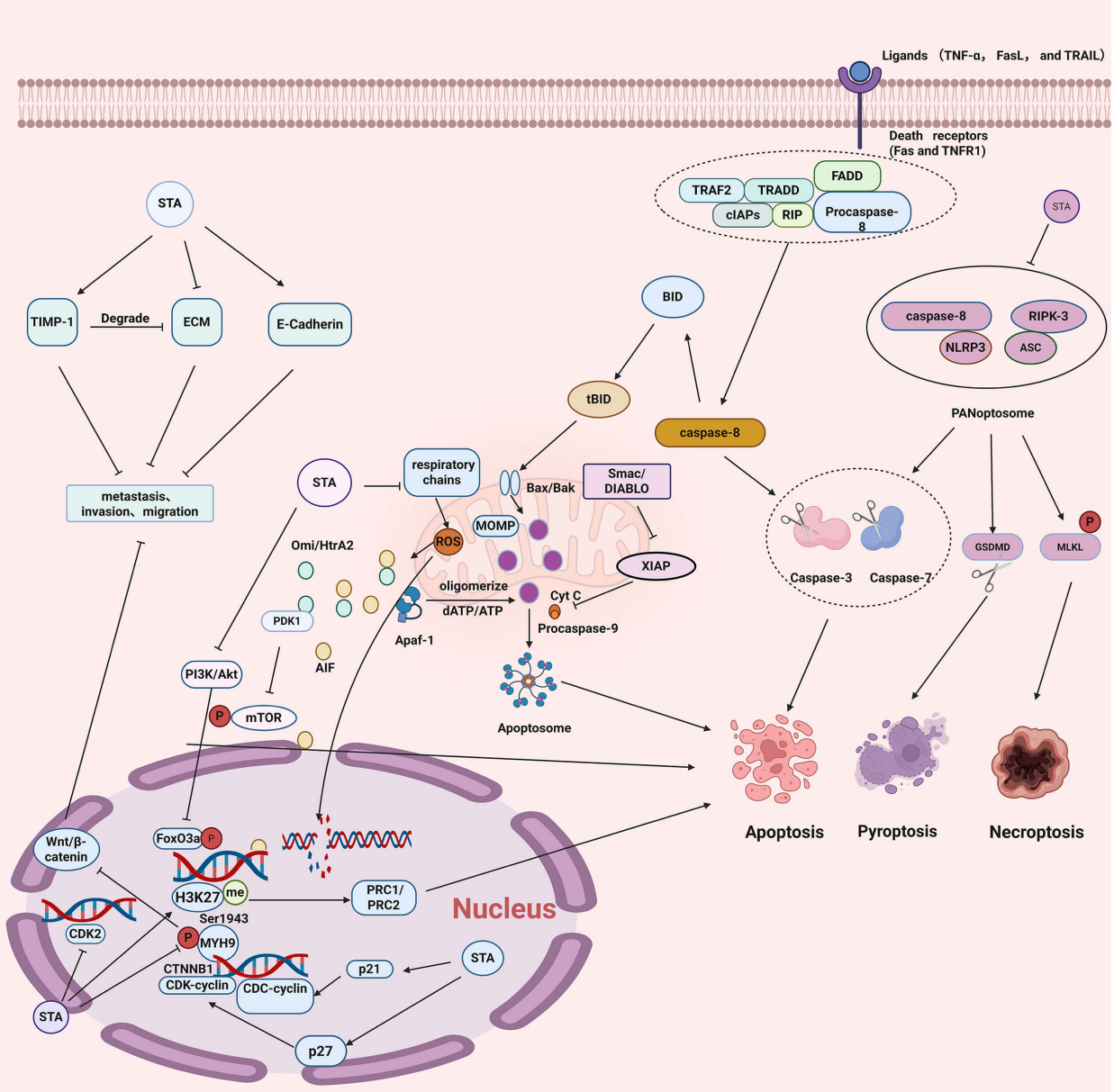

Fig. 2. Antitumor mechanisms of STA. AIF, apoptosis-inducing factor; Apaf-1, apoptotic peptidase activating factor 1; ASC, apoptosis-associated speck-like protein containing a CARD; Bax, BCL-2-associated X protein; Bak, BCL-2 antagonist/killer; BID, BH3-interacting domain death agonist; CDK, cyclin-dependent kinase; CTNNB1, catenin beta 1; Cyt C, cytochrome c; ECM, extracellular matrix; E-Cadherin, epithelial cadherin; FADD, Fas-associated death domain; FoxO3a, forkhead box O3a; GSDMD, gasdermin D; H3K27me, histone H3 lysine 27 methylation; MLKL, mixed lineage kinase domain-like protein; MOMP, mitochondrial outer membrane permeabilization; MYH9, myosin heavy chain 9; NLRP3, NOD-like receptor thermal protein domain associated protein 3; PDK1, 3-phosphoinositide-dependent protein kinase 1; PI3K, phosphatidylinositol 3-kinase; PRC1/2, polycomb repressive complex 1/2; RIP, receptor-interacting serine/threonine-protein kinase; RIPK3, receptor-interacting serine/threonine-protein kinase 3; ROS, reactive oxygen species; Smac/DIABLO, second mitochondria-derived activator of caspase / direct IAP-binding protein with low pI; TIMP-1, tissue inhibitor of metalloproteinase-1; TNF-α, tumor necrosis factor-α; TRAF2, TNF receptor-associated factor 2; TRADD, TNF receptor-associated death domain; TRAIL, TNF-related apoptosis-inducing ligand; XIAP, X-linked inhibitor of apoptosis protein. Solid arrows indicate activation or promotion; blunt-ended lines indicate inhibition. Created in BioRender. (2026) https://BioRender.com/y7jx2xo.

stage apoptosis. Because the caspase-independent pathway dominates the late stage and remains unaffected by Bcl-2, strategies that exclusively enhance caspase activity cannot completely block STA-induced cell death. Thus, combination regimens should target multiple pathways. Strikingly, STA confers a significant therapeutic advantage over conventional chemotherapeutic agents. Using a drug-resistant Jurkat T-cell subclone (designated JM319), Stepczynska

A and colleagues [24] demonstrated that although these cells exhibited complete refractoriness to various anticancer drugs, they retained profound sensitivity to STA-induced apoptosis. Notably, only STA triggered caspase activation and proteolytic cleavage of caspase substrates in these resistant cells, suggesting STA's potential to circumvent chemoresistance mechanisms in tumor cells [24].

Recent studies significantly advanced the understanding of STA-induced cell death modalities. A 2024 publication in the Journal of Biological Chemistry indicated that STA is not merely a non-lytic apoptosis inducer [25]. At low concentrations and short exposures, STA triggers classical apoptosis; however, prolonged treatment leads to PANoptosis, a highly inflammatory programmed cell death form incorporating apoptosis, necroptosis, and pyroptosis. Caspase-8 and receptor-interacting protein kinase 3 (RIPK3) form the PANoptosome complex core. These proteins interact to trigger dual outcomes: caspase-8 activates apoptosis through caspase-3/7 cleavage and simultaneously initiates pyroptosis via GSDMD cleavage. Conversely, RIPK3 induces necroptosis by phosphorylating mixed lineage kinase domain-like protein (MLKL). These converging pathways result in plasma membrane disruption, release of cellular contents, and extrusion of damage-associated molecular patterns (DAMPs), contrasting sharply with the non-lytic features of early apoptosis [26]. This finding suggests STA's antitumor effectiveness partially relies on immunogenic cell death (ICD), rather than simply removing malignant cells silently.

In hepatocellular carcinoma (HepG2 cells), STA regulates metabolic and survival signaling through mitochondrial pathways [27]. The mitochondrial serine protease Omi/HtrA2, released into the cytosol, binds and degrades phosphoinositide-dependent protein kinase-1 (PDK1), thereby inhibiting mTOR phosphorylation. This Omi/HtrA2-PDK1-PI3K/Akt axis functions independently of both ubiquitin-proteasome and autophagic degradation pathways. When the mTOR/Akt signaling pathway is inhibited, it suppresses cell proliferation and exerts this effect further by targeting ATP-binding cassette transporter A1 (ABCA1). Simultaneously, this inhibitory effect blocks ABCA1-mediated drug efflux by competing for ATP, promoting intracellular STA accumulation and thereby enhancing drug sensitivity [28]. Downstream, PI3K/Akt inhibition leads to forkhead box protein O3a (FoxO3a) dephosphorylation, enabling FoxO3a to bind the promoter region of p53-upregulated modulator of apoptosis (PUMA) and activate its transcription [29]. Importantly, this regulatory mechanism occurs independently of p53, providing therapeutic advantages in tumors harboring p53 mutations. Epigenetic regulation also represents an important dimension of STA-induced antitumor activity.

In osteosarcoma G292 cells, treatment with 1 μM STA for 3 hours selectively induced mono-, di-, and trimethylation of histone H3 lysine 27 (H3K27me1/me2/me3) without affecting H3K4 or H3K9 methylation. These histone modifications recruit Polycomb repressive complexes 1 and 2 (PRC1/PRC2) to silence pro-survival genes, thus driving apoptosis [30].

STA inhibits tumor cell motility in multiple solid tumors. In lung adenocarcinoma A549 cells, 24-hour treatment with 100 nM STA inhibited cellular adhesion and invasion by 74% and 54%, respectively [31]. This involved downregulation of adhesion molecules (laminin receptor and integrin β1) and upregulation of E-cadherin, restricting cell mobility and basement membrane degradation. In prostate cancer cells, STA notably increased tissue inhibitor of metalloproteinases-1 (TIMP-1), indirectly inhibiting extracellular matrix degradation, potentially associated with elevated interleukin-10 (IL-10) expression [32].

However, the effects of STA on tumor cell motility vary by cell type. In breast cancer studies, STA promoted single-cell migration in MCF-7 cells but inhibited migration in MDA-MB-231 and SK-BR-3 cells [33]. Collectively, all three cell lines demonstrated suppressed migration through distinct mechanisms, MCF-7 cells exhibited increased parallel-edge migration, whereas MDA-MB-231 and SK-BR-3 cells displayed significantly reduced migration velocity. Although transient ERK1/2 activation occurred in all cell lines, it was unrelated to migration regulation. This complexity suggests that STA's modulation of cell motility depends significantly on extracellular matrix conditions and tumor cell characteristics.

Recent investigations led by Ye G and colleagues [34] identified an unexpected intracellular target of STA, the nuclear non-muscle myosin heavy chain II-A (MYH9), which is markedly overexpressed in gastric cancer metastatic tissues. Mechanistically, MYH9 translocates into the nucleus via four nuclear localization signals (NLS), where its DNA-binding domain directly interacts with the CTNNB1 promoter and assembles a functional transcriptional complex with myosin light chain 9 (MYL9) and β-actin. This complex drives CTNNB1 transcription, activates the Wnt/β-catenin signaling cascade, and ultimately enhances anoikis resistance and invasive potential. STA specifically targets the phosphorylation of MYH9 at serine 1943 (Ser1943). By inhibiting this post-translational modification, STA disrupts the nuclear functional conformation of MYH9, impedes its binding to the CTNNB1 promoter and subsequent complex assembly, and consequently suppresses CTNNB1 transcription. This effectively reverses the hyperactivation of the Wnt/β-catenin pathway [35,36]. This finding identifies MYH9 Ser1943 phosphorylation as a novel target for treating gastric cancer peritoneal metastasis.

STA's anti-angiogenic activity was confirmed using chick chorioallantoic membrane assays and bovine carotid artery endothelial cell models. STA exhibited potent anti-angiogenic effects (*in vivo* ID_{50} = 71 pmol/egg; *in vitro* IC_{50} = 0.9 nM) [37]. Notably, STA did not significantly affect serum-induced endothelial migration, indicating that

its anti-angiogenic activity is primarily mediated through the suppression of endothelial cell proliferation rather than inhibition of migration. This feature may guide drug selection in combination anti-angiogenic therapy strategies.

3. Structural Optimization of STA Derivatives and Their Structure-Activity Relationships

The indolocarbazole scaffold forms the essential pharmacophore of STA, acting as a structural mimic of the ATP adenine base. It interacts with residues in the ATP-binding cleft of protein kinases via hydrophobic contacts and hydrogen bonds, competitively inhibiting nucleotide binding and thus blocking kinase-mediated phosphorylation cascades [38,39]. Maintaining this core scaffold while implementing targeted structural modifications allows the fine-tuning of physicochemical properties, including kinase affinity, cytotoxicity, tumor selectivity, and lipophilicity, to improve pharmacological activity and target specificity (Fig. 3). Utilizing this structural feature, recent medicinal chemistry efforts have focused on targeted modifications at the C-3′ amino position (via *N*-acylation), the C-7 position (through oxidation or hydroxylation), the C-3 position (via halogenation), and the glycosidic moiety (through sugar modification). These alterations significantly enhance antitumor efficacy, improve cellular targeting precision, reduce off-target toxicity, and introduce novel functional properties. Systematic elucidation of these SAR strategies and their mechanistic implications provides critical theoretical insights and practical guidelines for the rational design of next-generation STA-based antitumor agents characterized by enhanced potency, safety, and specificity.

Li K et al. [40] introduced an innovative paradigm for designing staurosporine-based fluorescent probes by constructing a donor–π–acceptor (D–π–A) electronic push-pull architecture. Cyanoacrylate-based electron-withdrawing moieties, specifically methyl cyanoacrylate [40], ethyl cyanoacetate, and isopropyl cyanoacetate, were strategically installed at the C-3 position of the indolocarbazole scaffold, yielding three novel derivatives: MCY-STA (Fig. 4, compound 7), ECY-STA (Fig. 4, compound 8), and ICY-STA (Fig. 4, compound 9). This approach elegantly circumvents the limitations of conventional fluorescent labeling methods, which typically introduce substantial steric hindrance and compromised polarity due to bulky fluorophores, consequently diminishing binding affinity to the ATP-binding cleft of kinases. By employing a conjugated π–bridge linking the electron-donating STA core to cyanoacrylate acceptors, the D–π–A architecture maximally preserves PKCθ binding capacity while conferring excellent fluorescent properties. Biological evaluation revealed that these derivatives exhibit potent sub-nanomolar inhibitory activity against PKCθ with IC_{50} values of 0.81 nM, 0.35 nM, and 1.13 nM, respectively, demonstrating superior antiproliferative efficacy compared with the parent compound against NCI-N87 (gastric), MCF-7 (breast), and SK-OV-3 (ovarian) cancer cell lines, achieving IC_{50} values below 1 μM. By integrating enhanced antitumor activity with fluorescence imaging capabilities, these STA-based fluorescent probes achieve combined diagnostic and therapeutic functions [41,42,43]. This breakthrough resolves the traditional trade-off between biomarker labeling and therapeutic activity, thereby opening new avenues for developing targeted therapeutics and bioimaging agents based on this marine natural product.

Systematic cytotoxicity profiling by Zhou et al. [44] demonstrated that compound 16 (Fig. 4) exhibits exceptional antiproliferative activity (IC_{50} = 9.99 nM) against colorectal adenocarcinoma SW-620 cells, approximately 2.5-fold greater potency than STA (IC_{50} = 25.10 nM). Although compounds 10–23 (Fig. 4) share relatively similar chemical structures, they exhibit significant differences in half-maximal inhibitory concentrations. For instance, compounds 10–13 (Fig. 4) demonstrate IC_{50} values in the micromolar range, whereas compound 16 shows nanomolar-level potency. Structural analyses revealed that the C5′–N12 bond configuration is a critical structural determinant of cytotoxic efficacy. Notably, the chemical structures of compounds 19 and 24 (Fig. 4) are highly similar, with compound 24 (Fig. 4) precisely resulting from the removal of the hydroxyl group at the 2′-position of compound 19 (Fig. 4). Previous studies demonstrated that compound 24 (Fig. 4) inhibits breast cancer cell migration [45]. These findings provide strategic guidance for structural optimization of STA derivatives and hold significant potential for developing novel STA-based antitumor drugs.

Li K et al. [40] performed additional structural optimization of staurosporine derivatives and evaluated their activities against seven cancer cell lines, including MV4-11, MCF-7, HCT-116, TE-1, PATU8988T, HOS, and GBC-SD. Specifically, compound 25 (Fig. 4), featuring a carbonyl modification at the C-7 position of midostaurin, exhibited potent antiproliferative activity against MV4-11 cells (IC_{50} = 0.078 ± 0.004 μM) and achieved a remarkably high selectivity index (SI = 1254), representing approximately a 3-fold improvement compared to midostaurin (SI = 405) [46]. Against human pancreatic cancer PATU8988T cells, compound 25 (Fig. 4) displayed an IC_{50} of 0.666 ± 0.055 μM and an SI of 147, markedly outperforming doxorubicin (IC_{50} = 1.118 μM, SI = 0.04). Further introduction of a halogen substituent at the 3-position of compound 25 (Fig. 4) yielded compound 26 (Fig. 4), which showed substantially enhanced selectivity. Against MCF-7 breast cancer cells, compound 26 (Fig. 4) achieved an IC_{50} of 0.029 ± 0.002 μM and an SI of 102, demonstrating superior inhibitory potency and selectivity compared to the positive controls UCN-01 (IC_{50} = 1.636 ± 0.281 μM, SI = 0.6) and doxorubicin (IC_{50} = 0.084 ± 0.034 μM, SI = 0.5).

Using combinatorial biosynthesis through heterologous expression of the engineered spc gene cluster in Strep-

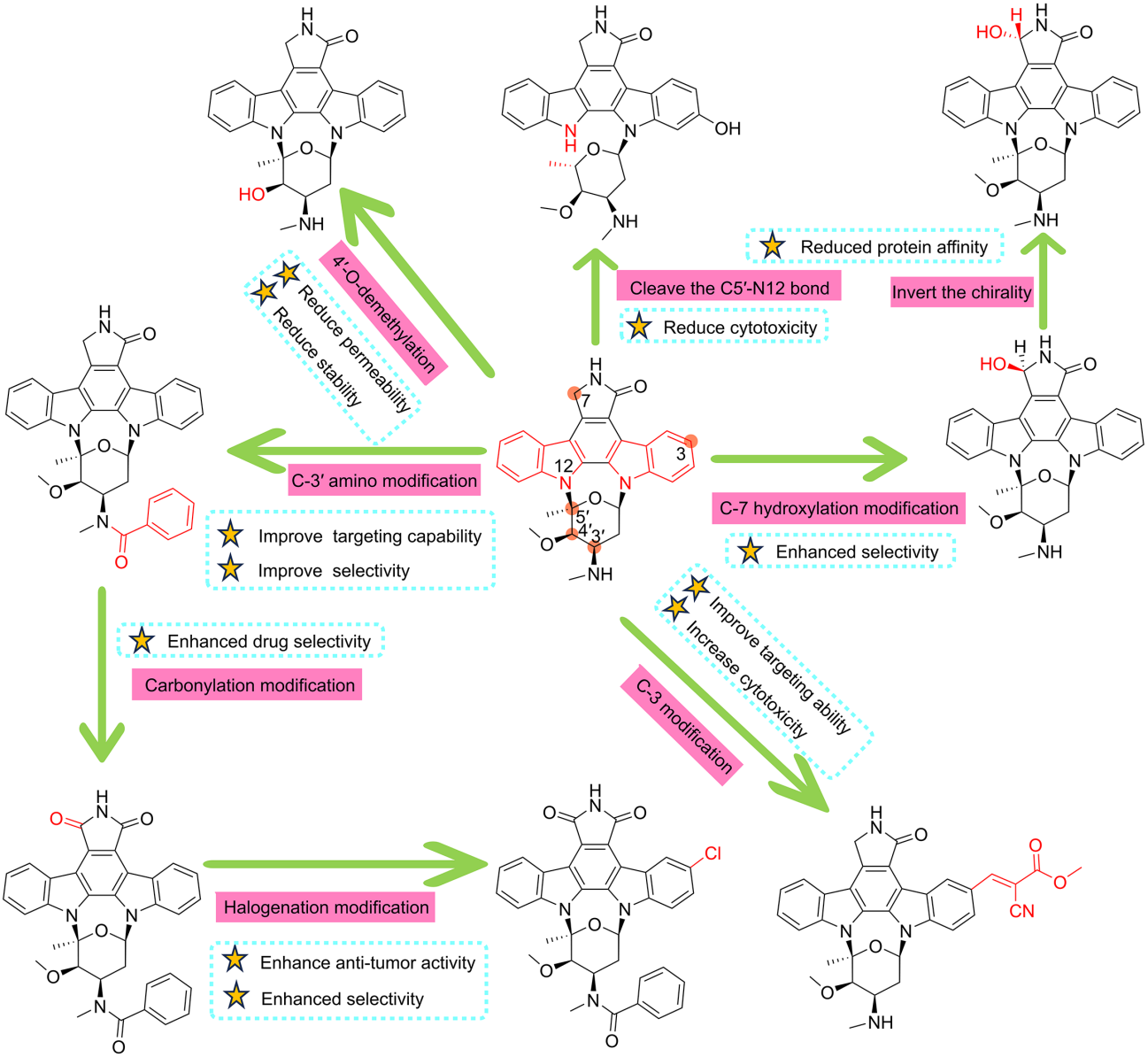

Fig. 3. The structure-activity relationship (SAR) of STA converting into derivatives.

tomyces coelicolor M1146, Xiao et al. [47] generated two novel STA derivatives alongside five known metabolites, assessing their cytotoxicity against HCT-116, K562, Huh7.5, and normal hepatic LO2 cells. Compounds 27, 28, 30, and 31 (Fig. 4) demonstrated potent antiproliferative activity and favorable therapeutic indices. Compound 29 (Fig. 4) selectively inhibited HCT-116 (IC_{50} = 2.7 μM) and K562 (IC_{50} = 8.8 μM) cells. Detailed SAR analysis indicated that the integrity of the C5′-N12 glycosidic bond, substitution patterns on the sugar amine, and pyrrole-acetyl modifications critically influence cytotoxicity and selectivity. Compound 27 (Fig. 4), possessing an intact C5′-N12 bond, exhibited 8- to 25-fold greater potency compared with its cleaved counterpart, compound 28 (Fig. 4). Intriguingly, compound 30 (Fig. 4) showed distinct selectivity (IC_{50} values of 2.1 μM and 24.2 μM against Huh7.5 and LO2 cells, respectively). In contrast, compound 29 (Fig. 4) displayed selective cytotoxicity: it showed negligible activity against both Huh7.5 and LO2 cells (IC_{50} >100 μM) but exerted significant efficacy against HCT-116 cells. Compared with compound 30 (Fig. 4), compound 29 (Fig. 4) bears a hydroxyl substitution at the C-9 position, which may explain this distinct cytotoxic profile. Compound 31 (Fig. 4) exhibited an excellent safety profile, displaying no hepatotoxicity at 100 μM, attributable to the presence of the 1-(1H-pyrrol-2-yl)ethanone group. These results demonstrate that combinatorial biosynthesis represents a green strategy to produce diverse STA analogs with improved cancer selectivity and reduced toxicity to normal cells, thus supporting the development of next-generation indolocarbazole drugs.

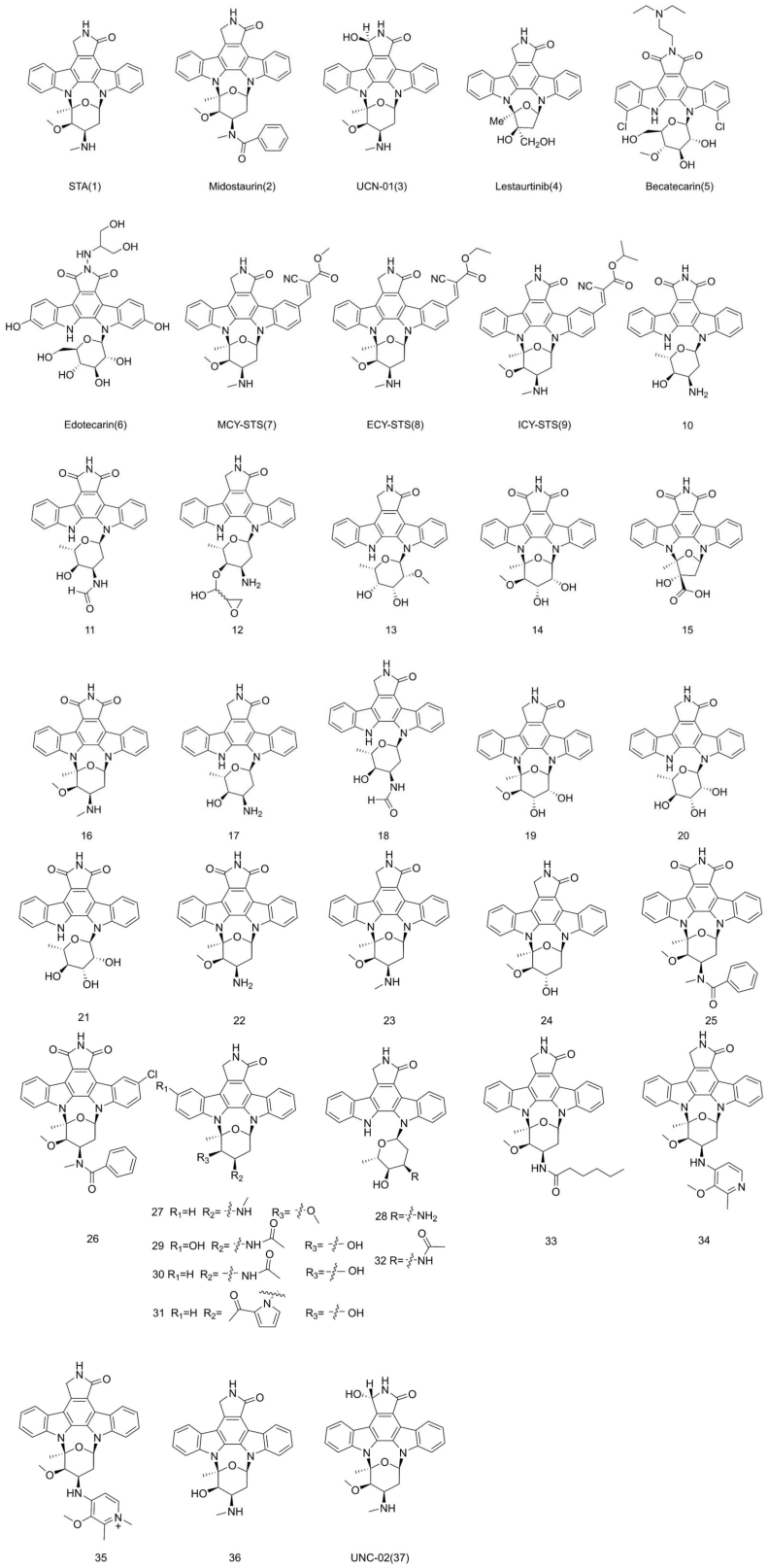

Fig. 4. Structural diagram of the compound.

Acylation at the C-3′ amino position converts broad-spectrum kinase inhibitors into targeted antineoplastic agents. Optimized derivatives selectively inhibit FLT3-ITD mutant AML cells (MV4-11; IC_{50} = 0.55–1.88 μM) while sparing normal hepatic (L-02) cells. The clinical success of midostaurin, characterized by improved PKC selectivity,

reduced systemic toxicity, and synergy with 5-fluorouracil (5-FU), highlights the therapeutic advantages of C-3′ amino acylation. This modification has become foundational for treating FLT3-mutated hematological malignancies [48].

Cui et al. [48] further validated C-3′ amino acylation as a critical strategy for improving target selectivity and minimizing off-target toxicity through compounds 33–35 (Fig. 4). Comprehensive antiproliferative assays across 12 human cancer cell lines, including lung, gastric, breast, and hematological malignancies, and normal hepatic L-02 cells demonstrated selective inhibition against FLT3-ITD mutant AML (MV4-11; IC_{50} values: 0.81 ± 0.007 μM, 0.55 ± 0.04 μM, 1.88 ± 0.11 μM). This targeted profile contrasts sharply with STA's broad kinase inhibition, substantially reducing cytotoxicity to normal cells. Midostaurin's clinical approval underscores the translational potential of this approach, demonstrating enhanced selectivity, safety, and synergy with chemotherapy (5-FU) [49]. Midostaurin is currently a first-line therapy for FLT3-mutated AML, highlighting targeted modulation of oncogenic drivers as critical to reducing dose-limiting toxicities and establishing C-3′ amino acylation as a cornerstone modification for clinical translation of indolocarbazole alkaloids [19].

Structural optimization of the STA scaffold inevitably involves strategic trade-offs between potency and selectivity, as systematically investigated by Yang et al. [50]. Based on the STA structure, the overall PKC inhibitory activity of compound 36 (Fig. 4), after removal of the 4′-O-methyl group, was reduced compared with the parent compound. However, this modification enhanced selectivity for specific PKC isoforms, making these analogs valuable pharmacological tools for dissecting subtype-specific signaling mechanisms and developing precision therapeutics. Conversely, retaining the 4′-O-methyl substituent is essential for maintaining robust target-binding affinity, metabolic stability, and cellular membrane permeability, pharmacokinetic properties critical for *in vivo* efficacy [12]. Consequently, methylation at the 4′-O position constitutes a pivotal structural determinant, balancing isoform selectivity and intrinsic biological potency, highlighting its crucial role in determining pharmacological activity and drug-like properties of indolocarbazole alkaloids.

The critical influence of stereochemistry on pharmacological properties is exemplified by the C-7 positional isomers of the indolocarbazole scaffold [47]. While both 7-hydroxystaurosporine (UCN-01) and its epimer UCN-02 (Fig. 4, compound 37) contain hydroxyl substituents at the C-7 position, they differ in absolute configuration; the former adopts the R-configuration, while the latter assumes the S-configuration. This subtle stereochemical divergence significantly affects their binding affinities to α_1-acid glycoprotein (AGP), a major plasma protein involved in drug distribution and pharmacokinetics. UCN-01 exhibits the highest binding affinity among this series, whereas STA demonstrates only approximately 5% of that binding capacity. Remarkably, inversion of the C-7 configuration from the R- to the S-enantiomer (UCN-01 to UCN-02) results in a greater than 100-fold reduction in AGP binding affinity [51]. These quantitative structure-binding relationships underscore stereochemistry as a critical determinant of molecular recognition processes, profoundly influencing drug-protein interactions and, consequently, the pharmacokinetic and pharmacodynamic profiles of indolocarbazole derivatives.

4. Mechanisms of Action of STA Derivatives

Using STA as a privileged lead scaffold, multiple research groups have successfully developed structurally novel derivatives with significant pharmacological potency and optimized drug-like properties. Representative clinical candidates include UCN-01, lestaurtinib, and the FDA-approved therapeutic agent midostaurin, among others (Table 1). These advances represent critical breakthroughs in medicinal chemistry and structure-based drug design, highlighting strong antitumor potential and offering new options for cancer therapy. Building upon this foundation, subsequent sections comprehensively discuss the molecular targets, signaling pathways, and pharmacodynamic profiles underlying the antitumor activities of these derivatives (Fig. 5 and Table 1).

4.1 Midostaurin

Midostaurin, a potent multi-target kinase inhibitor effective against both FLT3-ITD and FLT3-TKD mutant isoforms, has been established as a first-line therapeutic agent for FLT3-mutated AML. Mechanistically, midostaurin inhibits the PI3K/Akt/mTOR signaling cascade via FLT3 blockade, thereby inducing cytotoxicity through extensive inhibition of the mTOR pathway. Specifically, PI3K inhibition reduces downstream Akt and mTOR activities, leading to decreased phosphorylation of p70S6K and subsequent inhibition of mRNA translation. Concurrently, this disrupted signaling induces G1-phase cell cycle arrest, and suppresses malignant cell proliferation [52].

Complementing this mechanism, midostaurin-mediated FLT3 inhibition attenuates the RAS/RAF/MEK/ERK pathway, thereby decreasing ERK nuclear translocation and suppressing transcription of genes involved in proliferation and metastasis [53]. Additionally, midostaurin modulates chemotherapy resistance by inhibiting the ATP-binding cassette transporter ABCB1 (P-glycoprotein). Unlike conventional competitive inhibitors, midostaurin neither alters ABCB1 expression nor competes for drug-binding sites. Instead, it enhances chemotherapy sensitivity by reducing ABCB1 phosphorylation levels, thereby promoting apoptotic cell death in leukemia cells [54,55,56]. Moreover, midostaurin demonstrates comparable efficacy in reversing resistance to vinblastine and doxorubicin [57]. Furthermore, midostaurin exerts antileukemic effects by regulating the

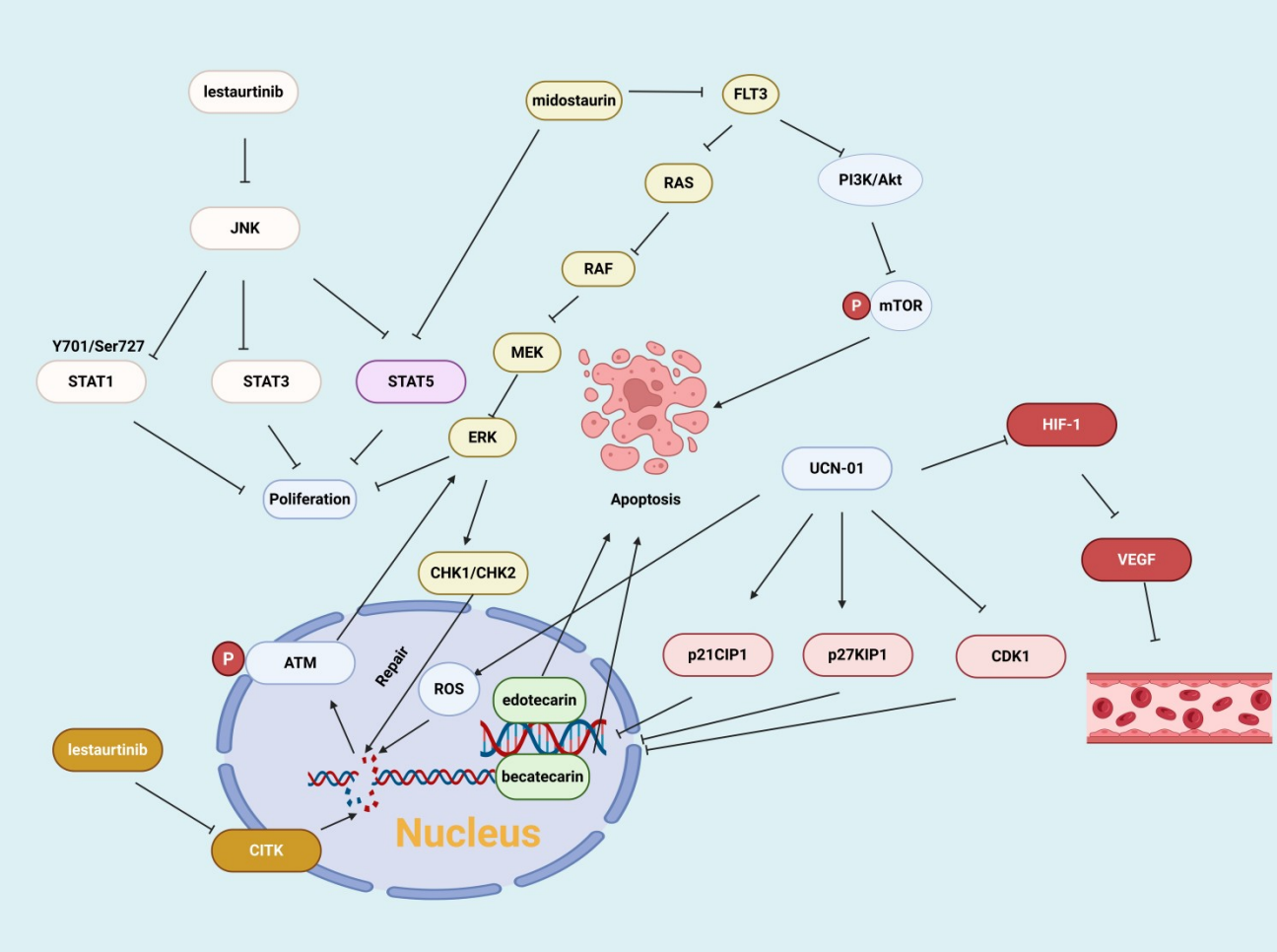

Fig. 5. Antitumor mechanisms of midostaurin, UCN-01, lestaurtinib, becatecarin, and edotecarin. ATM, Ataxia-telangiectasia mutated; CHK1/CHK2, Checkpoint kinase 1/2; CITK, Citron kinase; ERK, Extracellular regulated protein kinase; FLT3, FMS-like tyrosine kinase 3; HIF-1, Hypoxia-inducible factor-1; JNK, c-Jun N-terminal kinase; MEK, Mitogen-activated protein kinase kinase; mTOR, Mammalian target of rapamycin; PI3K, Phosphatidylinositol 3-kinase; RAF, Rapidly accelerated fibrosarcoma; RAS, Rat sarcoma viral oncogene homolog; ROS, Reactive oxygen species; STAT1, Signal transducer and activator of transcription 1; STAT3, Signal transducer and activator of transcription 3; STAT5, Signal transducer and activator of transcription 5; VEGF, Vascular endothelial growth factor; p21CIP1, Cyclin-dependent kinase inhibitor 1A; p27KIP1, Cyclin-dependent kinase inhibitor 1B; CDK1, Cyclin-dependent kinase 1. Solid arrows indicate activation or promotion; blunt-ended lines indicate inhibition. Created in BioRender. (2026) https://BioRender.com/cyoxs6c.

STAT5 signaling pathway, further contributing to its comprehensive therapeutic profile.

However, recent studies indicate that midostaurin as a monotherapy has minimal clinical efficacy in AML treatment [58]. Research demonstrates that combining midostaurin with sphingosine kinase-1 (SK-1) inhibitors (SKI-II or resveratrol) effectively reverses resistance by inhibiting the activation and phosphorylation of FLT3 and STAT5A. This combination overcomes resistance, enhances tumor cell sensitivity to midostaurin, and significantly improves antitumor efficacy [59,60]. Currently, clinical practice frequently employs midostaurin in combination with other anticancer agents to maximize therapeutic outcomes [61].

4.2 UCN-01

UCN-01 possesses a unique pharmacological property termed "cytostatic protection" characterized by induction of specific and reversible G1-phase cell cycle arrest in normal proliferating cells while sparing malignant cells with defective checkpoint machinery (Fig. 5 and Table 1) [62]. This differential modulation of the cell cycle is therapeutically valuable in oncology, especially for breast cancer treatment, by selectively protecting normal tissues from chemotherapy-induced cytotoxicity without compromising the antineoplastic efficacy of cytotoxic agents. Mechanistically, low-dose UCN-01 specifically targets the intact G0/G1 checkpoint in normal cells, inducing transient cytostasis through the upregulation of cyclin-dependent ki-

Table 1. Targets and clinical applications of STA derivatives.

Compounds	Structures	Targets	Indications/clinical studies
midostaurin	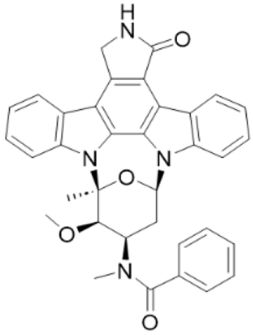	FLT3	AML
UCN-01 (7-hydroxystaurosporine)	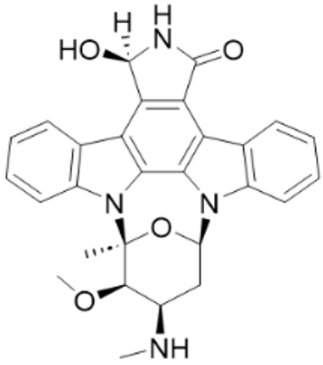	HIF-1	AML, Solid tumor
lestaurtinib	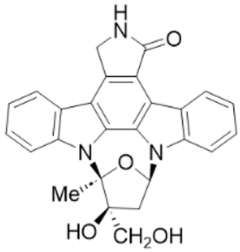	CITK, STAT1/3	AML, ALL
becatecarin	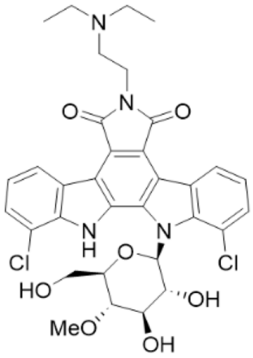	Topo I/II	SCLC, CRC
edotecarin	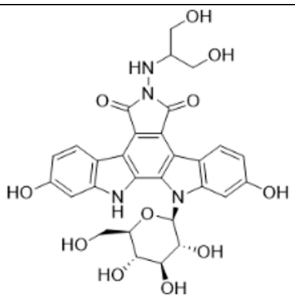	Topo I	CRC, GBM

FLT3, FMS-like tyrosine kinase 3; AML, acute myeloid leukemia; CITK, Citron kinase; SCLC, small cell lung cancer; HIF-1, Hypoxia inducible factor-1; STAT1/3, Signal transducer and activator of transcription 1/3; ALL, Acute lymphoblastic leukemia; CRC, Colorectal cancer; GBM, Glioblastoma; Topo I/II, Topoisomerase I/II.

nase inhibitors p21CIP1 and p27KIP1, along with simultaneous downregulation of CDK1 kinase activity. This action results in cell cycle pause without damaging genomic integrity. In contrast, tumor cells harboring defective G0/G1 checkpoints fail to respond to the same low-dose stimulation, bypassing arrest signals and continuing uncontrolled proliferation. Paradoxically, this enhances their sensitivity to cytotoxic agents while normal tissues remain protected. Experimental validation in murine intestinal epithelial models confirms that a single low dose of 5 mg/kg UCN-01 induces substantial proliferation arrest in intestinal crypt cells within 24 hours. This effect persists for approximately 7 days, with complete restoration of normal proliferative capacity observed by 14 days post-treatment. Notably, preclinical studies in tumor-bearing mice have shown that administration of 5-FU after pretreatment with a low dose of UCN-01 can reduce chemotherapy toxicity [62]. Thus, exploiting the disparities in cell cycle checkpoint function between normal and malignant tissues establishes an effective therapeutic strategy for selective chemoprotection.

Lien et al. [63] identified a distinct cytotoxic mechanism of UCN-01 in U2-OS osteosarcoma cells. The compound induces metabolic hyperactivation and significant accumulation of reactive oxygen species (ROS), resulting in oxidative DNA double-strand breaks (DSBs) [63]. This genotoxic stress triggers ATM autophosphorylation at Ser1981 and activates ERK signaling, initiating the canonical DNA damage response (DDR) via downstream effectors CHK1 and CHK2. Paradoxically, UCN-01 simultaneously disrupts CHK1/CHK2-mediated signaling, effectively disabling the G2/M DNA damage checkpoint despite persistent upstream ATM activation. Consequently, tumor cells containing unrepaired DNA damage bypass the critical G2 repair checkpoint and forcibly enter mitosis. This leads to chromosomal fragmentation, segregation defects, and mitotic catastrophe, ultimately resulting in apoptotic cell death. Concomitantly, Lien et al. [63] demonstrated that UCN-01 potently inhibits osteosarcoma cell migration. Short-term exposure to subtoxic concentrations significantly reduces cellular motility, as demonstrated by wound healing assays, without impairing cell viability. Mechanistically, this anti-migratory effect results from disruption of the nuclear-centrosome-Golgi axis orientation. Specifically, UCN-01 treatment induces loss of Golgi ribbon polarity and structural integrity. Microtubule regrowth assays confirmed that the compound inhibits microtubule nucleation, a crucial step in establishing the anteroposterior polarity axis. Consequently, UCN-01-induced structural disorganization eliminates directional persistence, effectively preventing directed cell migration and metastatic potential.

UCN-01 demonstrates a bifunctional anti-angiogenic mechanism at clinically achievable concentrations (<100–200 nM), concurrently suppressing endothelial cell proliferation and inhibiting the pro-angiogenic responses of tumor cells to hypoxic stress [64]. In the rat aortic ring assay, concentrations as low as 32 nM effectively block neovascularization by suppressing hypoxia-inducible HIF-1 transcriptional activity and subsequent VEGF secretion under hypoxic conditions [64,65]. This targeted disruption of hypoxia-driven angiogenesis indicates that the antineoplastic efficacy of UCN-01 at sub-cytotoxic concentrations primarily results from indirect inhibition of tumor vascularization rather than direct tumor cell killing, thereby providing a distinct therapeutic approach centered on microenvironmental modulation.

4.3 Lestaurtinib

Using RNA sequencing and functional gene knockout experiments, Rodman et al. [66] identified STAT1 and STAT3 as essential drivers of ovarian cancer cell proliferation. Lestaurtinib achieves antineoplastic effects through a dual-mechanism approach. It concurrently inhibits the JNK and ERK signaling pathways, thereby blocking STAT1 and STAT3 phosphorylation at both tyrosine (Y701/705) and serine (S727) residues, terminating proliferative signals. Simultaneously, it strongly suppresses JAK/STAT signaling. This comprehensive blockade of STAT activation, targeting both tyrosine and serine phosphorylation, provides deeper and more complete suppression of the JAK/STAT axis compared to ruxolitinib, an FDA-approved agent that exclusively inhibits tyrosine phosphorylation. Furthermore, cell cycle and apoptosis analyses revealed that lestaurtinib rapidly induces cell cycle arrest, followed by progressive apoptotic cell death, demonstrating potent antiproliferative efficacy at clinically achievable concentrations.

Pinto et al. [67] evaluated lestaurtinib as a therapeutic candidate for anaplastic thyroid cancer (ATC), demonstrating potent antiproliferative activity with nanomolar IC_{50} values across ATC cell lines. Mechanistically, lestaurtinib suppresses JAK2-mediated signaling by inhibiting STAT5 phosphorylation, thereby disrupting downstream proliferative signals. Rather than inducing apoptosis, lestaurtinib exerts cytostatic effects via G2/M cell cycle arrest. In chick chorioallantoic membrane xenograft models, treatment with 4 μM lestaurtinib significantly reduced tumor growth compared with vehicle controls. Additionally, anti-angiogenic activity was confirmed by power Doppler ultrasonography. Collectively, these findings reveal a dual mechanism involving both antiproliferative and anti-angiogenic effects, providing a preclinical rationale for developing lestaurtinib as a targeted therapy for ATC.

Pallavicini et al. [68] clarified the multifaceted antineoplastic mechanism of lestaurtinib in medulloblastoma, identifying Citron kinase (CITK) as the primary molecular target and demonstrating concurrent activation of multiple tumor-suppressive pathways. Mechanistically, lestaurtinib directly inhibits CITK kinase activity with an IC_{50} of 90 nM, thereby preventing phosphorylation of the substrate inner centromere protein. This inhibition results in defective late cytokinesis, G0/G1 cell cycle arrest, and accumu-

lation of DNA double-strand breaks, indicated by increased 53BP1 foci, elevated γH2AX levels, and decreased RAD51 expression. These genomic insults ultimately lead to mitotic catastrophe and activate TP53 superfamily-dependent stress responses, resulting in p21 induction and caspase-3-mediated apoptosis. The central role of CITK inhibition was confirmed through rescue experiments demonstrating that CITK overexpression attenuates lestaurtinib's antiproliferative effects. The lack of additive effects following CITK knockdown further confirms on-target specificity. In the SmoA1 transgenic mouse medulloblastoma model, weekly intratumoral administration of 100 nM lestaurtinib effectively induced apoptosis, inhibited tumor progression, and significantly prolonged survival with minimal toxicity to normal brain tissue. These findings establish a favorable therapeutic window and support its promising clinical translation.

4.4 Edotecarin

Edotecarin, a novel indolocarbazole-derived topoisomerase I (Top I) inhibitor, exhibits a potent and tightly regulated mechanism of action distinct from that of direct DNA-damaging agents. Rather than directly inducing genotoxic lesions, Edotecarin stabilizes the Top I-DNA cleavable complex, thereby selectively inhibiting the religation step of the Top I catalytic cycle and preventing the resolution of transient DNA single-strand breaks [69]. This sustained enzymatic inhibition leads to the accumulation of unresolved single-strand breaks, ultimately triggering replication-associated cytotoxicity and apoptotic tumor cell death.

Edotecarin demonstrates superior DNA cleavage efficiency compared with NB-506 and conventional camptothecin, preferentially targeting C/T-G sequences with a potent IC_{50} of 0.05 μM [69]. Notably, its cytotoxic activity is independent of cell cycle phase, showing comparable efficacy in both actively proliferating and quiescent G0/G1-phase tumor cells. Moreover, Edotecarin exhibits high selectivity for topoisomerase I, with minimal activity against topoisomerase II. This selectivity reduces non-specific genomic injury and limits toxicity to normal tissues, thereby conferring a favorable safety profile for clinical application.

4.5 Becatecarin

Becatecarin, a water-soluble derivative of rebeccamycin, acts as a dual topoisomerase I/II (Top I/II) inhibitor with potent antineoplastic activity [8,70]. Its mechanism involves stabilization of the Top I/II-DNA cleavable complex, thereby blocking DNA religation, arresting replication forks, and promoting DSBs. These events result in cell cycle arrest and apoptotic cell death. In addition, becatecarin can intercalate into DNA, further enhancing its cytotoxic effects. In Phase I/II clinical trials, becatecarin administered daily for five consecutive days demonstrated clinical activity in both SCLC and non-small cell lung cancer. Sequential inhibition of topoisomerase I and II enhances antitumor efficacy and provides a strategic advantage in overcoming resistance mechanisms.

5. Conclusion

Given the escalating global cancer burden, characterized by increasing incidence and mortality rates, the development of effective antineoplastic agents remains an urgent clinical priority. This review systematically outlines the diverse antitumor mechanisms of STA and its synthetic derivatives. These mechanisms include the inhibition of tumor cell proliferation, the induction of apoptotic cell death, the suppression of tumor cell migration and invasion, and the reduction of tumor angiogenesis. Furthermore, the analysis provides detailed insights into SAR, clarifying how specific chemical modifications modulate pharmacological potency and target selectivity. Collectively, these findings provide a robust theoretical foundation for the rational design and clinical development of next-generation targeted anticancer drugs.

STA, a marine-derived natural scaffold, provides a versatile structural platform. Through structural optimization, it can be transformed from a broadly cytotoxic compound into clinically viable candidates with enhanced target selectivity and improved safety profiles. This strategy offers distinct advantages in overcoming chemoresistance and augmenting antitumor efficacy. Current structural modification strategies for STA primarily focus on specific sites, including the C-3′ amino acylation group, the C-7 position, the C5′-N12 position, and the C-3 position, whereas research on other positions remains limited. Although the STA derivative midostaurin has achieved significant progress in leukemia treatment, its efficacy against solid tumors remains unsatisfactory due to multitarget activity, suboptimal selectivity, and marked interindividual variability. Apart from midostaurin, which has been applied in leukemia therapy, other STA derivatives discussed in this study have failed to achieve selective single-target inhibition and frequently exhibit drug resistance, ultimately failing to meet clinical requirements despite entering clinical trials. These limitations pose significant challenges to the broader application of STA-based antitumor agents. For instance, the first-generation FLT3 inhibitor lestaurtinib progressed into clinical trials but ultimately failed due to insufficient therapeutic efficacy [71]. The primary limitation arises from unfavorable pharmacokinetic properties, particularly high plasma protein binding, which limits the free drug fraction available for target engagement. Additionally, substantial interpatient variability in steady-state plasma concentrations hampers consistent target inhibition across patient populations [72]. However, these setbacks provide critical insights that inform subsequent rational design strategies and optimization efforts for next-generation STA-based anticancer drugs.

Future research efforts, guided by previous developmental challenges and existing pharmacological limitations, should adopt a clinically driven approach. Comprehensive mechanistic investigations and rational structural optimization of staurosporine derivatives are required to overcome existing deficiencies and enhance therapeutic potential. The integration of advanced drug delivery systems, such as nanoparticles, liposomes, and micelles, offers promising strategies to improve pharmacokinetic properties and facilitate penetration of the blood-brain barrier, thereby addressing bioavailability limitations [73]. Current studies have demonstrated that liposomal encapsulation of STA exhibits effective anticancer activity with minimal side effects in mouse models [74]. Furthermore, the application of fluorescent probe technologies and combinatorial biosynthesis methods enables real-time tumor imaging and structural diversification, thereby providing a strong foundation for the development of precision-targeted anticancer therapeutics. Notably, future studies will integrate PROTAC-based probe technologies for target discovery, aiming to systematically identify previously unexplored antitumor targets of STA [75]. This approach will further elucidate its mechanisms of action and accelerate the development of novel anticancer therapies.

The successful regulatory approval of the STA derivative midostaurin, significant clinical advancements with UCN-01, and lessons derived from the development of lestaurtinib and related analogues collectively demonstrate ongoing therapeutic progress. These cumulative experiences offer a solid basis for anticipating the emergence of next-generation STA derivatives characterized by enhanced safety profiles, improved target selectivity, and clearly defined clinical efficacy. Such advances hold considerable promise for expanding the arsenal of precision oncology therapies, providing novel therapeutic strategies for cancer patients in the foreseeable future.

Author Contributions

Writing–original draft, Conceptualization: SJL, SY, GSZ, WJH. Writing–review & editing, Supervision, Funding acquisition, Conceptualization: SLQ. All authors have participated sufficiently in the work and agreed to be accountable for all aspects of the work. All authors read and approved the final manuscript.

Ethics Approval and Consent to Participate

Not applicable.

Acknowledgment

We extend our sincere gratitude to all individuals who provided assistance during manuscript preparation, as well as to the Chawdraw and BioRender software for their support in figure generation. We also appreciate the valuable guidance and recommendations provided by all reviewers.

Funding

This research was funded by the Hunan Science Fund for Distinguished Young Scholars (No. 2025JJ20098) and the National Natural Science Foundation of China (No. 82204250).

Conflicts of Interest

The authors declare no conflicts of interest.

References

[1] Dee EC, Wu JF, Feliciano EJG, Ting FIL, Willmann J, Ho FDV, et al. National Cancer System Characteristics and Global Pan-Cancer Outcomes. JAMA Oncology. 2025; 11: 650–654. https://doi.org/10.1001/jamaoncol.2025.0473

[2] Xie J, Yang Z, Zhou C, Zhu J, Lee RJ, Teng L. Nanotechnology for the delivery of phytochemicals in cancer therapy. Biotechnology Advances. 2016; 34: 343–353. https://doi.org/10.1016/j.biotechadv.2016.04.002

[3] Chen W, Shi K, Yu Y, Yang P, Bei Z, Mo D, et al. Drug delivery systems for colorectal cancer chemotherapy. Chinese Chemical Letters. 2024; 35: 109159. https://doi.org/10.1016/j.cclet.2023.109159

[4] Lee D, Kim Y, Kang DH, Chung C. Modeling Drug and Radiation Resistance with Patient-Derived Organoids: Recent Progress, Unmet Needs, and Future Directions for Lung Cancer. Cells. 2025; 14: 1994. https://doi.org/10.3390/cells14241994

[5] Baltussen JC, de Glas NA, van Holstein Y, van der Elst M, Trompet S, Uit den Boogaard A, et al. Chemotherapy-Related Toxic Effects and Quality of Life and Physical Functioning in Older Patients. JAMA Network Open. 2023; 6: e2339116. https://doi.org/10.1001/jamanetworkopen.2023.39116

[6] Malve H. Exploring the ocean for new drug developments: Marine pharmacology. Journal of Pharmacy & Bioallied Sciences. 2016; 8: 83–91. https://doi.org/10.4103/0975-7406.171700

[7] Mayer AMS, Pierce M, Reji M, Wu AC, Jekielek KK, Le HQ, et al. Marine-Derived Pharmaceuticals in Clinical Trials in 2022. The Journal of Pharmacology and Experimental Therapeutics. 2023; 385: 299. https://doi.org/10.1124/jpet.122.527010

[8] Xu M, Bai Z, Xie B, Peng R, Du Z, Liu Y, et al. Marine-Derived Bisindoles for Potent Selective Cancer Drug Discovery and Development. Molecules. 2024; 29: 933. https://doi.org/10.3390/molecules29050933

[9] Tao X, Wang H, Wang Q, Wang C, Shao CW, Jin Y, et al. Marine Natural Product Chagosendine C Induces Cuproptosis in Colorectal Cancer Cells by Targeting FDX1. Journal of the American Chemical Society. 2025; 147: 37089–37103. https://doi.org/10.1021/jacs.5c07917

[10] Santos FC, Marquês JT, Santos EN, de Almeida RFM. Staurosporine as an Antifungal Agent. International Journal of Molecular Sciences. 2025; 26: 9683. https://doi.org/10.3390/ijms26199683

[11] Bu S, Wang Y, Yin W, Wen Q, Wang P, Zhu W. Staurosporine Natural Products Derived from Marine Streptomyces sp. OUCMDZ-5522. Chinese Journal of Organic Chemistry. 2025; 45: 2486–2500. https://doi.org/10.6023/cjoc202411022

[12] Nakano H, Omura S. Chemical biology of natural indolocarbazole products: 30 years since the discovery of staurosporine. The Journal of Antibiotics. 2009; 62: 17–26. https://doi.org/10.1038/ja.2008.4

[13] Gayler KM, Kong K, Reisenauer K, Taube JH, Wood JL. Staurosporine Analogs Via C-H Borylation. ACS Medicinal Chemistry Letters. 2020; 11: 2441–2445. https://doi.org/10.1021/acsmedchemlett.0c00420

[14] Gescher A. Analogs of staurosporine: potential anticancer drugs? General Pharmacology: The Vascular System. 1998; 31: 721–728. https://doi.org/10.1016/s0306-3623(98)00069-x
[15] Sausville EA, Arbuck SG, Messmann R, Headlee D, Bauer KS, Lush RM, et al. Phase I trial of 72-hour continuous infusion UCN-01 in patients with refractory neoplasms. Journal of Clinical Oncology. 2001; 19: 2319–2333. https://doi.org/10.1200/JCO.2001.19.8.2319
[16] Knapper S, Burnett AK, Littlewood T, Kell WJ, Agrawal S, Chopra R, et al. A phase 2 trial of the FLT3 inhibitor lestaurtinib (CEP701) as first-line treatment for older patients with acute myeloid leukemia not considered fit for intensive chemotherapy. Blood. 2006; 108: 3262–3270. https://doi.org/10.1182/blood-2006-04-015560
[17] Schwandt A, Mekhail T, Halmos B, O'Brien T, Ma PC, Fu P, et al. Phase-II trial of rebeccamycin analog, a dual topoisomerase-I and -II inhibitor, in relapsed "sensitive" small cell lung cancer. Journal of Thoracic Oncology. 2012; 7: 751–754. https://doi.org/10.1097/JTO.0b013e31824abca2
[18] Goel S, Wadler S, Hoffman A, Volterra F, Baker C, Nazario E, et al. A phase II study of rebeccamycin analog NSC 655649 in patients with metastatic colorectal cancer. Investigational New Drugs. 2003; 21: 103–7. https://doi.org/10.1023/a:1022980613420
[19] Xu M, Peng R, Min Q, Hui S, Chen X, Yang G, et al. Bisindole natural products: A vital source for the development of new anticancer drugs. European Journal of Medicinal Chemistry. 2022; 243: 114748. https://doi.org/10.1016/j.ejmech.2022.114748
[20] Harmalkar MN, Shirsat NV. Staurosporine-induced growth inhibition of glioma cells is accompanied by altered expression of cyclins, CDKs and CDK inhibitors. Neurochemical Research. 2006; 31: 685–692. https://doi.org/10.1007/s11064-006-9068-0
[21] Baltuch GH, Dooley NP, Couldwell WT, Yong VW. Staurosporine differentially inhibits glioma versus non-glioma cell lines. Journal of Neuro-oncology. 1993; 16: 141–147. https://doi.org/10.1007/BF01324701
[22] Malsy M, Bitzinger D, Graf B, Bundscherer A. Staurosporine induces apoptosis in pancreatic carcinoma cells PaTu 8988t and Panc-1 via the intrinsic signaling pathway. European Journal of Medical Research. 2019; 24: 5. https://doi.org/10.1186/s40001-019-0365-x
[23] Zhang XD, Gillespie SK, Hersey P. Staurosporine induces apoptosis of melanoma by both caspase-dependent and -independent apoptotic pathways. Molecular Cancer Therapeutics. 2004; 3: 187–197. https://doi.org/10.1158/1535-7163.187.3.2
[24] Stepczynska A, Lauber K, Engels IH, Janssen O, Kabelitz D, Wesselborg S, et al. Staurosporine and conventional anticancer drugs induce overlapping, yet distinct pathways of apoptosis and caspase activation. Oncogene. 2001; 20: 1193–1202. https://doi.org/10.1038/sj.onc.1204221
[25] Sarkar R, Choudhury SM, Kanneganti TD. Classical apoptotic stimulus, staurosporine, induces lytic inflammatory cell death, PANoptosis. The Journal of Biological Chemistry. 2024; 300: 107676. https://doi.org/10.1016/j.jbc.2024.107676
[26] Yu Z, Jiang N, Su W, Zhuo Y. Necroptosis: A Novel Pathway in Neuroinflammation. Frontiers in Pharmacology. 2021; 12: 701564. https://doi.org/10.3389/fphar.2021.701564
[27] Ding Y, Wang B, Chen X, Zhou Y, Ge J. Staurosporine suppresses survival of HepG2 cancer cells through Omi/HtrA2-mediated inhibition of PI3K/Akt signaling pathway. Tumour Biology. 2017; 39: 1010428317694317. https://doi.org/10.1177/1010428317694317
[28] Yang Q, Gao W, Li X, Li X, Zhou X, Li W, et al. Targeting ABCA1 via Extracellular Vesicle-Encapsulated Staurosporine as a Therapeutic Strategy to Enhance Radiosensitivity. Advanced Healthcare Materials. 2024; 13: e2400381. https://doi.org/10.1002/adhm.202400381
[29] Asadi Y, Moundounga RK, Chakroborty A, Pokokiri A, Wang H. FOXOs and their roles in acute and chronic neurological disorders. Frontiers in Molecular Biosciences. 2025; 12: 1538472. https://doi.org/10.3389/fmolb.2025.1538472
[30] Cheng MF, Lee CH, Hsia KT, Huang GS, Lee HS. Methylation of histone H3 lysine 27 associated with apoptosis in osteosarcoma cells induced by staurosporine. Histology and Histopathology. 2009; 24: 1105–11. https://doi.org/10.14670/hh-24.1105
[31] Wang Y, Yang H, Liu H, Huang J, Song X. Effect of staurosporine on the mobility and invasiveness of lung adenocarcinoma A549 cells: an in vitro study. BMC Cancer. 2009; 9: 174. https://doi.org/10.1186/1471-2407-9-174
[32] Tachibana K, Shimizu T, Tonami K, Takeda K. Staurosporine enhances the expression of tissue inhibitor of metalloproteinase-1 in human prostate cancer cells. Biochemical and Biophysical Research Communications. 2002; 295: 489–494. https://doi.org/10.1016/s0006-291x(02)00704-0
[33] Meyer FAH, Kraus D, Glassmann A, Veit N, Winter J, Probstmeier R. The Presence of Yin-Yang Effects in the Migration Pattern of Staurosporine-Treated Single versus Collective Breast Carcinoma Cells. International Journal of Molecular Sciences. 2021; 22: 11961. https://doi.org/10.3390/ijms222111961
[34] Ye G, Yang Q, Lei X, Zhu X, Li F, He J, et al. Nuclear MYH9-induced CTNNB1 transcription, targeted by staurosporin, promotes gastric cancer cell anoikis resistance and metastasis. Theranostics. 2020; 10: 7545–7560. https://doi.org/10.7150/thno.46001
[35] Zeng XF, Wang YW, Ou Y, Liu L. Role of myosin heavy chain 9 in gastrointestinal tumorigenesis: A comprehensive review. World Journal of Gastrointestinal Oncology. 2025; 17: 106617. https://doi.org/10.4251/wjgo.v17.i6.106617
[36] Feroz W, Park BS, Siripurapu M, Ntim N, Kilroy MK, Sheikh AMA, et al. Non-Muscle Myosin II A: Friend or Foe in Cancer? International Journal of Molecular Sciences. 2024; 25: 9435. https://doi.org/10.3390/ijms25179435
[37] Oikawa T, Shimamura M, Ashing H, Nakamura O, Kanayasu T, Morita I, et al. Inhibition of angiogenesis by staurosporine, a potent protein kinase inhibitor. The Journal of Antibiotics. 1992; 45: 1155–1160. https://doi.org/10.7164/antibiotics.45.1155
[38] Xu ZB, Chaudhary D, Olland S, Wolfrom S, Czerwinski R, Malakian K, et al. Catalytic domain crystal structure of protein kinase C-theta (PKCtheta). The Journal of Biological Chemistry. 2004; 279: 50401–50409. https://doi.org/10.1074/jbc.M409216200
[39] Prade L, Engh RA, Girod A, Kinzel V, Huber R, Bossemeyer D. Staurosporine-induced conformational changes of cAMP-dependent protein kinase catalytic subunit explain inhibitory potential. Structure. 1997; 5: 1627–1637. https://doi.org/10.1016/s0969-2126(97)00310-9
[40] Li K, Liu W, Wu T, Wei Y, Liu Y, Zhou J, et al. Natural Staurosporine Derivatives with Fluorescence for Cancer Theranostics. ChemMedChem. 2025; 20: e202500629. https://doi.org/10.1002/cmdc.202500629
[41] Wang X, Chen N, Wei Y, Zhou J, Chen M, Xu H, et al. Design and application of staurosporine-based AIE fluorescent probes. Materials Letters. 2025; 399: 139047. https://doi.org/10.1016/j.matlet.2025.139047
[42] Wang X, Chen N, Zhang L, Chen X, Zhou J, Zhang X, et al. Staurosporine Scaffold-Based AIE-Active Molecules with Photo-Isomerization and Bioactive Properties: Applications in Subcellular Organelle Targeting. ChemistrySelect. 2025; 10: e03316. https://doi.org/10.1002/slct.202503316
[43] Chen N, Ye Y, Zhang L, Wang X, Liu S, Chen X, et al. The development of novel AIE-active staurosporine-based fluorescent

probes with theranostic potential. New Journal of Chemistry. 2026; 50: 1982–1989. https://doi.org/10.1039/d5nj03817k
[44] Zhou B, Hu ZJ, Zhang HJ, Li JQ, Ding WJ, Ma ZJ. Bioactive staurosporine derivatives from the Streptomyces sp. NB-A13. Bioorganic Chemistry. 2019; 82: 33–40. https://doi.org/10.1016/j.bioorg.2018.09.016
[45] Chen RY, Ding LJ, Liu YJ, Shi JJ, Yu J, Li CY, et al. Marine Staurosporine Analogues: Activity and Target Identification in Triple-Negative Breast Cancer. Marine Drugs. 2024; 22: 459. https://doi.org/10.3390/md22100459
[46] Li G, Wu D, Xu Y, He W, Wang D, Zhu W, et al. Synthesis and Antitumor Activity of Staurosporine Derivatives. Natural Product Communications. 2022; 17: 1–6. https://doi.org/10.1177/1934578x221103036
[47] Xiao F, Li H, Xu M, Li T, Wang J, Sun C, et al. Staurosporine Derivatives Generated by Pathway Engineering in a Heterologous Host and Their Cytotoxic Selectivity. Journal of Natural Products. 2018; 81: 1745–1751. https://doi.org/10.1021/acs.jnatprod.8b00103
[48] Cui T, Lin S, Wang Z, Fu P, Wang C, Zhu W. Cytotoxic Indolocarbazoles From a Marine-Derived *Streptomyces* Sp. OUCMDZ-5380. Frontiers in Microbiology. 2022; 13: 957473. https://doi.org/10.3389/fmicb.2022.957473
[49] Eder JP, Jr, Garcia-Carbonero R, Clark JW, Supko JG, Puchalski TA, Ryan DP, et al. A phase I trial of daily oral 4'- N - benzoyl-staurosporine in combination with protracted continuous infusion 5-fluorouracil in patients with advanced solid malignancies. Investigational New Drugs. 2004; 22: 139–150. https://doi.org/10.1023/B:DRUG.0000011790.31292.ef
[50] Yang SW, Lin LJ, Cordell GA, Wang P, Corley DG. O- and N-methylation in the biosynthesis of staurosporine. Journal of Natural Products. 1999; 62: 1551–1553. https://doi.org/10.1021/np990261q
[51] Landin EJB, Williams C, Ryan SA, Bochel A, Akter N, Redfield C, et al. The structural basis for high affinity binding of α1-acid glycoprotein to the potent antitumor compound UCN-01. The Journal of Biological Chemistry. 2021; 297: 101392. https://doi.org/10.1016/j.jbc.2021.101392
[52] Weisberg E, Meng C, Case AE, Tiv HL, Gokhale PC, Buhrlage SJ, et al. Effects of the multi-kinase inhibitor midostaurin in combination with chemotherapy in models of acute myeloid leukaemia. Journal of Cellular and Molecular Medicine. 2020; 24: 2968–2980. https://doi.org/10.1111/jcmm.14927
[53] Gallogly MM, Lazarus HM, Cooper BW. Midostaurin: a novel therapeutic agent for patients with FLT3-mutated acute myeloid leukemia and systemic mastocytosis. Therapeutic Advances in Hematology. 2017; 8: 245–261. https://doi.org/10.1177/2040620717721459
[54] Sucha S, Sorf A, Svoren M, Vagiannis D, Ahmed F, Visek B, et al. ABCB1 as a potential beneficial target of midostaurin in acute myeloid leukemia. Biomedicine & Pharmacotherapy. 2022; 150: 112962. https://doi.org/10.1016/j.biopha.2022.112962
[55] Beltran PJ, Fan D, Fidler IJ, O'Brian CA. Chemosensitization of cancer cells by the staurosporine derivative CGP 41251 in association with decreased P-glycoprotein phosphorylation. Biochemical Pharmacology. 1997; 53: 245–247. https://doi.org/10.1016/s0006-2952(96)00718-6
[56] Sedlak J, Hunakova L, Duraj J, Chorvath B, Novotny L. Effects of protein kinase C inhibitor, staurosporine derivative CGP 41 251, on cell cycle, DNA synthesis and drug uptake in neoplastic cell lines. Anti-cancer Drugs. 1995; 6: 70–76. https://doi.org/10.1097/00001813-199502000-00008
[57] Utz I, Spitaler M, Rybczynska M, Ludescher C, Hilbe W, Regenass U, et al. Reversal of multidrug resistance by the staurosporine derivatives CGP 41251 and CGP 42700. International Journal of Cancer. 1998; 77: 64–69. https://doi.org/10.1002/(sici)1097-0215(19980703)77:1%3C64::aid-ijc11%3E3.0.co;2-9
[58] Levis M. Midostaurin approved for FLT3-mutated AML. Blood. 2017; 129: 3403–3406. https://doi.org/10.1182/blood-2017-05-782292
[59] Tecik M, Adan A. Concurrent inhibition of FLT3 and sphingosine kinase-1 triggers synergistic cytotoxicity in midostaurin resistant FLT3-ITD positive acute myeloid leukemia cells via blocking FLT3/STAT5A signaling to induce apoptosis. Journal of Chemotherapy. 2026; 38: 145–161. https://doi.org/10.1080/1120009X.2025.2478340
[60] Tecik M, Adan A. Functional combination of resveratrol and midostaurin induces cytotoxicity to overcome acquired midostaurin resistance in FLT3-ITD expressing acute myeloid leukemia cells. Naunyn-Schmiedeberg's Archives of Pharmacology. 2026; 399: 2275–2289. https://doi.org/10.1007/s00210-025-04543-8
[61] Rörby E, Adolfsson J, Hultin E, Gustafsson T, Lotfi K, Cammenga J, et al. Multiplexed single-cell mass cytometry reveals distinct inhibitory effects on intracellular phosphoproteins by midostaurin in combination with chemotherapy in AML cells. Experimental Hematology & Oncology. 2021; 10: 7. https://doi.org/10.1186/s40164-021-00201-w
[62] Mull BB, Livingston JA, Patel N, Bui T, Hunt KK, Keyomarsi K. Specific, reversible G1 arrest by UCN-01 in vivo provides cytostatic protection of normal cells against cytotoxic chemotherapy in breast cancer. British Journal of Cancer. 2020; 122: 812–822. https://doi.org/10.1038/s41416-019-0707-z
[63] Lien WC, Chen TY, Sheu SY, Lin TC, Kang FC, Yu CH, et al. 7-hydroxy-staurosporine, UCN-01, induces DNA damage response, and autophagy in human osteosarcoma U2-OS cells. Journal of Cellular Biochemistry. 2018; 119: 4729–4741. https://doi.org/10.1002/jcb.26652
[64] Kruger EA, Blagosklonny MV, Dixon SC, Figg WD. UCN-01, a protein kinase C inhibitor, inhibits endothelial cell proliferation and angiogenic hypoxic response. Invasion & Metastasis. 1998; 18: 209–218. https://doi.org/10.1159/000024514
[65] Spyridopoulos I, Luedemann C, Chen D, Kearney M, Chen D, Murohara T, et al. Divergence of angiogenic and vascular permeability signaling by VEGF: inhibition of protein kinase C suppresses VEGF-induced angiogenesis, but promotes VEGF-induced, NO-dependent vascular permeability. Arteriosclerosis, Thrombosis, and Vascular Biology. 2002; 22: 901–906. https://doi.org/10.1161/01.atv.0000020006.89055.11
[66] Rodman EPB, Emch MJ, Hou X, Bajaj A, Pearson NA, John AJ, et al. Lestaurtinib's antineoplastic activity converges on JAK/-STAT signaling to inhibit treatment naïve and therapy resistant forms ovarian cancer. NPJ Precision Oncology. 2025; 9: 236. https://doi.org/10.1038/s41698-025-00947-0
[67] Pinto N, Prokopec SD, Vizeacoumar F, Searle K, Lowerison M, Ruicci KM, et al. Lestaurtinib is a potent inhibitor of anaplastic thyroid cancer cell line models. PloS One. 2018; 13: e0207152. https://doi.org/10.1371/journal.pone.0207152
[68] Pallavicini G, Iegiani G, Parolisi R, Ferraro A, Garello F, Bitonto V, et al. Lestaurtinib inhibits Citron kinase activity and medulloblastoma growth through induction of DNA damage, apoptosis and cytokinesis failure. Frontiers in Oncology. 2023; 13: 1202585. https://doi.org/10.3389/fonc.2023.1202585
[69] Saif MW, Diasio RB. Edotecarin: a novel topoisomerase I inhibitor. Clinical Colorectal Cancer. 2005; 5: 27–36. https://doi.org/10.3816/ccc.2005.n.014
[70] Manda S, Mauser C, Bokar J, Cooney M, Brell J, Krishnamurthi S, et al. Phase I trial of combination becatecarin and oxaliplatin in patients with advanced solid tumors. Journal of Clinical Oncology. 2007; 25: 2561. https://doi.org/10.1200/jco.2007.25.18_suppl.2561
[71] Knapper S, Russell N, Gilkes A, Hills RK, Gale RE, Cavenagh

JD, et al. A randomized assessment of adding the kinase inhibitor lestaurtinib to first-line chemotherapy for FLT3-mutated AML. Blood. 2017; 129: 1143–1154. https://doi.org/10.1182/blood-2016-07-730648

[72] Young DJ, Nguyen B, Li L, Higashimoto T, Levis MJ, Liu JO, et al. A method for overcoming plasma protein inhibition of tyrosine kinase inhibitors. Blood Cancer Discovery. 2021; 2: 532–547. https://doi.org/10.1158/2643-3230.BCD-20-0119

[73] Bor G, Hosta-Rigau L. Next Generation of Brain Cancer Nanomedicines to Overcome the Blood–Brain Barrier (BBB): Insights on Transcytosis, Perivascular Tumor Growth, and BBB Models. Advanced Therapeutics. 2023; 6: 2300161. https://doi.org/10.1002/adtp.202300161

[74] Mukthavaram R, Jiang P, Saklecha R, Simberg D, Bharati IS, Nomura N, et al. High-efficiency liposomal encapsulation of a tyrosine kinase inhibitor leads to improved in vivo toxicity and tumor response profile. International Journal of Nanomedicine. 2013; 8: 3991–4006. https://doi.org/10.2147/ijn.s51949

[75] Yan S, Zhang G, Luo W, Xu M, Peng R, Du Z, et al. PROTAC technology: From drug development to probe technology for target deconvolution. European Journal of Medicinal Chemistry. 2024; 276: 116725. https://doi.org/10.1016/j.ejmech.2024.116725